HHS Public Access

Author manuscript

J Bone Miner Res. Author manuscript; available in PMC 2017 August 09.

Published in final edited form as:

J Bone Miner Res. 2017 August ; 32(8): 1692–1702. doi:10.1002/jbmr.3159.

Exercise Decreases Marrow Adipose Tissue Through ß-Oxidation in Obese Running Mice

Maya Styner[1], **Gabriel M Pagnotti**[2], **Cody McGrath**[1], **Xin Wu**[1], **Buer Sen**[1], **Gunes Uzer**[1,3], **Zhihui Xie**[1], **Xiaopeng Zong**[4], **Martin A Styner**[5,6], **Clinton T Rubin**[2], and **Janet Rubin**[1]

[1]Department of Medicine, Division of Endocrinology and Metabolism, University of North Carolina, Chapel Hill, NC, USA

[2]Department of Biomedical Engineering, State University of New York, Stony Brook, Stony Brook, NY, USA

[3]Department of Mechanical and Biomedical Engineering, Boise State University, Boise, ID, USA

[4]Department of Radiology and Biomedical Research Imaging Center, University of North Carolina, Chapel Hill, NC, USA

[5]Department of Computer Science, University of North Carolina, Chapel Hill, NC, USA

[6]Department of Psychiatry, University of North Carolina, Chapel Hill, NC, USA

Abstract

The relationship between marrow adipose tissue (MAT) and bone health is poorly understood. We used running exercise to ask whether obesity-associated MAT can be attenuated via exercise and whether this correlates with gains in bone quantity and quality. C57BL/6 mice were divided into diet-induced obesity (DIO, $n = 14$) versus low-fat diet (LFD, $n = 14$). After 3 months, 16-week-old mice were allocated to an exercise intervention (LFD-E, DIO-E) or a control group (LFD, DIO) for 6 weeks (4 groups, $n = 7$/group). Marrow adipocyte area was 44% higher with obesity ($p<0.0001$) and after exercise 33% lower in LFD ($p<0.0001$) and 39% lower in DIO ($p<0.0001$). In LFD, exercise did not affect adipocyte number; however, in DIO, the adipocyte number was 56% lower ($p<0.0001$). MAT was 44% higher in DIO measured by osmium-µCT, whereas exercise associated with reduced MAT (–23% in LFD, –48% in DIO, $p<0.05$). MAT was additionally quantified by 9.4TMRI, and correlated with osmium-µCT ($r = 0.645$; $p<0.01$). Consistent with higher lipid beta oxidation, *perilipin 3* (*PLIN3*) rose with exercise in tibial mRNA (+92% in LFD, +60% in DIO, $p<0.05$). Tibial µCT-derived trabecular bone volume (BV/TV) was not influenced by DIO but responded to exercise with an increase of 19% ($p<0.001$). DIO was associated with

Address correspondence to: Maya Styner, MD, University of North Carolina, Department of Medicine, Division of Endocrinology, CB 7170, 5002 Burnett Womack, 160 Dental Circle, Chapel Hill, NC 27599-7170, USA. mstyner@med.unc.edu.

Additional Supporting Information may be found in the online version of this article.

Disclosures

Dr. Styner has nothing to disclose.

Authors' roles: Study design: MS, CTR, and JR. Study conduct: MS, GMP, CM, XZ, and XW. Data collection: MS, GMP, CM, XW, and XZ. Data analysis: MS, CM, and MAS. Data interpretation: MS, GMP, CM, BS, GU, ZX, and MAS. Drafting manuscript: MS, GMP, and JR. Revising manuscript content: MS, GMP, CM, GU, MAS, CTR, and JR. Approving final version of manuscript: MS, GMP, and JR. MS takes responsibility for the integrity of the data analysis.

higher cortical periosteal and endosteal volumes of 15% ($p = 0.012$) and 35% ($p<0.01$), respectively, but Ct. Ar/Tt.Ar was lower by 2.4% ($p<0.05$). There was a trend for higher stiffness (N/m) in DIO, and exercise augmented this further. In conclusion, obesity associated with increases in marrow lipid—measured by osmium-μCT and MRI—and partially due to an increase in adipocyte size, suggesting increased lipid uptake into preexisting adipocytes. Exercise associated with smaller adipocytes and less bone lipid, likely invoking increased ß-oxidation and basal lipolysis as evidenced by higher levels of *PLIN3*.

Keywords

BONE; MEDICAL IMAGE ANALYSIS; MARROW ADIPOSE TISSUE; OBESITY; EXERCISE

Introduction

More than one-third of US adults are obese.[1] Obese individuals exhibit a preserved or even increased bone density, perhaps representing an adaptation to increased weight-based mechanical loading[2–6] or increased estrogen available through aromatization.[7,8] Similarly, in rodents, we and others have demonstrated that short-term high-fat feeding is associated with preserved or increased bone density.[9–11] There are studies that support a negative impact of obesity on bone quantity[12–14] or its biomechanical properties,[15,16] leading to the thinking that, despite increased bone quantity in the setting of obesity, bone quality and composition may not be commensurate to body weight, even representing relative bone fragility and increased fracture risk.[17,18] Further, obesity has been associated with increased fractures, albeit not classic osteoporotic fragility fractures.[19–21] Beyond the controversy of whether obesity is beneficial or harmful for bone health, the effect of localized "obesity" *within* bone, as represented by marrow adipose tissue (MAT), on bone health is controversial.[10,13,22–26]

Although it is clear that obesity increases white adipose cell size and number in extra-marrow fat depots,[27] the relationship between obesity and MAT cellularity is not known. We previously showed that MAT lipid volume increases rapidly during high-fat feeding in rodents relative to the total bone volume, rising earlier than calorie induction of visceral fat depot size.[5] A positive association between obesity and MAT has also been noted in humans[28] as well as rodents.[10] What remains unclear is whether adipocyte hypertrophy or hyperplasia accounts for increased MAT in the setting of calorie excess.

MAT accumulation due to high-fat diet (HFD) or PPARγ agonist is suppressed by daily exercise in mice.[22,29] Exercise suppression of MAT expansion occurs simultaneously with new bone formation.[30] Mechanical loading in mice has been shown to increase bone formation rates in loaded tibias.[31] Many rodent studies confirm increased bone formation rate as an adaptive response to exercise via histomorphometry,[32] including running exercise.[32] This process, besides requiring energy for muscular contraction, will also require energy for local bone formation. As such, the question of whether exercise utilizes marrow fat as an energy depot remains to be addressed.

In this study, we ask whether exercise is able to modulate MAT due to obesity in mice, building on prior work demonstrating the ability of exercise to modulate MAT after short-term HFD feeding. We additionally ask whether bone quantity and quality are affected by diet-induced obesity (DIO) and whether exercise can reverse effects on bone associated with obesity. Mice are used to answer these mechanistic questions regarding the physiologic relevance of MAT because sophisticated methods to quantify whole bone MAT (volumetrically) are not yet available in humans. By measuring MAT via established and additional methods in mice, we confirm that MAT is higher in the setting of DIO. We additionally validate MRI for volumetric quantification of MAT and correlate this with established methods in our laboratory. We will show that exercise can suppress MAT under both control and DIO conditions. Importantly, this exercise effect is correlated with a diminution in adipocyte size in both control and DIO. mRNA analysis of whole tibias confirms that DIO was associated with higher lipid storage. *Perilipin 3* (*PLIN3*) rose in exercised mice, consistent with an increase in ß-oxidation[33] and basal lipolysis.[34] Biomechanical strength of the tibia was higher in exercisers because of augmentation of cortical and trabecular thickness. Exercise was associated with improved resistance to bending in both diet groups, with a greater impact on bones from obese mice compared with those from non-obese mice.

Materials and Methods

Animals and diet

All procedures were IACUC approved. Four-week-old C57BL/6 female mice (The Jackson Laboratory, Bar Harbor, ME, USA) were housed in controlled light and temperature conditions. Animals were randomly divided into two groups and fed high-fat diet (HFD) of $n = 14$ versus low-fat diet (LFD) of $n = 14$. The mice were fed their assigned diet for a 3-month period, with the high-fat diet consisting of 45% of calories from fat (#D12451, Research Diets, New Brunswick, NJ, USA) and the low-fat diet consisting of 10% of calories from fat (#D12450B, Research Diets). Body weight was measured biweekly. In addition to this experimental group, a baseline control group ($n = 10$/diet group) was harvested before the initiation of exercise intervention. The mice were housed in groups of 2 or 3 before exercise intervention. During the exercise intervention, mice were individually housed to allow access to and use of running wheels.

Exercise intervention

After a 3-month dietary lead-in, 16-week-old mice in both diet groups were allocated to an exercise intervention for 6 weeks. The groups were as follows: 1) sedentary mice fed with a LFD (LFD group, $n = 7$); 2) running mice fed with LFD (LFD-E group, $n = 7$); 3) sedentary mice fed with a HFD (DIO group, $n = 7$); 4) running mice fed with a HFD (DIO-E group, $n = 7$). Access to the voluntary, running wheel was provided to exercise intervention groups as previously described.[35] Wheel use was monitored using a Mity 8 Cyclocomputer (model CC-MT400, CAT EYE, Ltd, Osaka, Japan).

Body composition

MRI technology was used to evaluate whole body composition (including fat, lean tissue, and water) in *vivo* 3 weeks after initiation of exercise intervention. Body composition was assessed using MRI (EchoMRI, Houston, TX, USA) to determine fat and lean mass percentages as previously described.[36]

Volumetric quantification and imaging of MAT by osmium-μCT

Osmium staining of lipid in mouse bones has been previously described.[22,29,37] Briefly, femurs were fixed, then decalcified and subsequently incubated with 1% osmium tetroxide/ 2.5% potassium dichromate for 48 hours. μCT imaging was performed at 10-μm isotropic resolution. Quantitative, volumetric image analysis[22,29] of the lipid binder, osmium was performed via standard-density (Hounsfield unit [HU]) weighted volumetric measurements. Only locations with a minimal density of 2000 HU were incorporated in the analysis.[22]

Imaging was performed via μCT with energy of 55 kVp, integration time of 500 ms, and resolution of 0.01×0.01×0.01 mm (Scanco μCT-35, Scanco Medical, Bruttisellen, Switzerland). Raw, unaligned femur images were first rigidly aligned (3D Slicer, www.slicer.org)[38] to present all images in a consistent fashion and to allow for superimposition of images. Bone masks were created next, starting from segmentation via standardized bone thresholds. Manual contouring was performed to outline the femur in all images to designate a total femoral volume (Insight-SNAP, www.itksnap.org).[39] Because osmium is significantly denser than bone, HU thresholds were set for visualization of osmium as follows: low osmium from 2000 to 3000 HU (red), mid osmium from 3000 to 4000 HU (green), and high osmium from 4000 to 5000 HU (blue). The lower threshold for osmium was chosen to be considerably above the HU for dense cortical bone.[40] The contribution of potentially mislabeled cortical bone to the osmium volume is expected to be negligible.[41] The maximal threshold of 5000 HU was chosen by inspecting the 99th percentile over the full image intensities. In between the lower and upper thresholds, we divided the osmium attenuation range into three uniformly separated categories.

Osmium within the bone mask was then quantified as volumetric (mm^3) measurements of low, mid, and high osmium stain regions in the femur. Osmium volume was normalized to total femoral volume TV (as % of TV). We reported and analyzed the % osmium (osmium in mm^3/total volume) above the mid osmium threshold of 3000 HU. Aligned femoral images were averaged across all images to form an average femur image as a reference for bone visualization. Images were also averaged within each group separately for color-coded visualizations of the osmium densities to allow for visual comparisons of MAT between groups (as in Fig. 2).

Volumetric quantification and imaging of MAT by MRI

Femurs were analyzed with a 9.4T horizontal small-bore MRI scanner. Water and fat maps were obtained with a 2- dimensional RARE imaging sequence with the following parameters: RARE factor = 4, TE = 28 ms, TR = 4000 ms, number of averages = 4, number of slices = 24, slice thickness = 0.5 mm, in-plane resolution = 100×100 μm^2, matrix size = 130×130. Utilizing the fact that the fat and water protons have a NMR frequency separation

of 3.5 ppm, a Gaussian-shaped 90° saturation pulse with a width of 2ms was applied preceding the RARE sequence to suppress the fat or water signal while leaving the other signal unaffected. The fat and water images were acquired by setting the saturation pulse frequency to be the same as the water and fat frequencies, respectively. In our processing workflow, we first manually subdivided the full images containing all 10 samples into individual images for each bone. Then, we employed the water images to manually outline femoral bone masks using Insight SNAP.[39] Using these bone masks, interior bone regions were masked from other image parts in both the water and fat maps. Next, we established a common, study-specific reference space by computing an unbiased average image[42] from the masked water maps using the ANTS registration software.[43] All individual water and fat maps were then propagated into the common space, where voxel-wise correspondence allows direct comparison of intensities. Average fat maps for each group were computed in the common space and superimposed on the common, average water image for visualization of group fat maps. Fat map intensities were represented with a colored heat map in 3D Slicer[39] for visualization (Fig. 2*C*). For MAT quantification, we created a regional label map of the femur, excluding cortical bone regions, with regions for the epiphysis, metaphysis, and diaphysis. Intensity-weighted volume of MAT was then quantified via the regional fat histograms akin to the MAT volumetric quantification in the osmium-μCT images.

Marrow adipocyte diameter and number quantification via histology

Fixed and decalcified femurs were imbedded in paraffin, sectioned into 5 μm slices, and stained with hematoxylin as previously described.[44] Imaging was performed on an Olympus X81 at 4× and 40× magnifications. The 40× magnification images were obtained at the distal femoral growth plate, where lipid content is maximal. ImageJ was used to isolate adipocytes within 40× images and to quantify adipocyte size as described in Parlee and colleagues.[45] Additionally, globular maxima were removed manually to isolate defined adipocytes. The “Analyze Particles” function was used to outline cells and calculate area, in pixels, for each (Supplemental Fig. S1*B*). A lower limit of 1000 pixels was applied. This process was applied to 3 images per slice, with 4 slices per mouse (mice analyzed per group: LFD, $n = 4$; LFD-E, $n = 4$; DIO, $n = 3$; DIO-E, $n = 4$), resulting in $n = 36–48$ images analyzed per group. Adipocyte number was obtained via ImageJ.[46] The marrow cavity from the metaphysis in the 4× magnification images were isolated. The area of the total white space within this isolated area was normalized to the average adipocyte area of that experimental group to obtain the total number of adipocytes within the image. This value was normalized to the total area of metaphysis isolated to obtain average adipocyte per square micrometer.

Bone microarchitecture

Bone microarchitecture parameters of the proximal tibial metaphysis and mid-diaphysis were quantified *ex vivo* as previously described (resolution = 12 μm, E = 55 kVa, I = 145 μA).[29,47–49] Intracortical porosities were quantified as previously described.[29] Cortical area is the area of cortical bone, whereas total area is total area enclosed by the periosteal bone surface (outer surface of the bone). Endosteal volume is the volume enclosed by the inner surface of the bone, and periosteal volume is the volume inside the outer surface of the

bone. These values represent the volumetric equivalent of the marrow area and the total area, respectively.

Biomechanical testing

Biomechanical testing was performed as previously described.[50,51] Briefly, the MTS 858 Minibionix II (MTS, Eden Prairie, MN, USA) was used to resolve the mechanical properties at the mid-diaphysis. For the 4-point bending: 50 kN load cell samples were placed across two struts (distance = 0.6 mm) with the anterior side facing up. Two struts fixed to the lowering piston (distance = 0.15 mm) were lowered at a constant rate (0.2 mm/s) across the mid-diaphysis until the sample was brought to ultimate failure. Parameters evaluated were stiffness, defined as the slope of the curve (force versus displacement) across the elastic region, ultimate strength (point-of-failure), and Young's modulus.

Real-time PCR

Total RNA was isolated from the whole tibia and 1 μg was reverse-transcribed and analyzed via real-time PCR. Ten microliters of cDNA from each experimental condition were pooled and diluted 1:10 to 1:10,000 to generate a 5-point standard curve. A non-template control was added to each PCR reaction. Standards and samples were run in duplicate. PCR products were normalized to GAPDH.

Statistical analysis

Statistical significance was evaluated by two-way ANOVA with correction for multiple comparisons via a Tukey post-hoc test (GraphPad Prism 7.0, GraphPad, La Jolla, CA, USA). Exercise and dietary intervention were used as the analysis variables. Our data sets passed the Shapiro-Wilk normality test (GraphPad Prism 7.0). The p value cut-off for significance is defined at less than or equal to 0.05. Trend is defined as a p value greater than 0.05 and less than 0.15. For Fig. 3, GraphPad Prism was used to analyze the histogram with generation of a Gaussian-fit curve.

Results

Exercise reduces fat mass

DIO mice weighed 14% more than those fed LFD (Fig. 1*A*, diet effect $p<0.001$, Supplemental Fig. S3). Fat mass measured by MRI 3 weeks before harvest was 35% higher in the DIO groups compared with LFD ($p<0.01$, Fig 1*C*). Fat pad weight at harvest correlated with fat mass, noted to be 129% higher in DIO compared with LFD ($p<0.0001$, Fig. 1*F*). Lean mass was higher by 7% in DIO compared with LFD and was unaffected by exercise in either dietary group ($p<0.01$, Fig. 1*E*). In humans, a body mass index (BMI) cut-off is used to define obesity (BMI>30); in mice, however, there is no predefined cut-off and, thus, body composition and weight are utilized to determine if an obese phenotype is present. Diet-induced obesity is an accepted mouse model of obesity,[52] but there is significant variation of weight response because of various factors: strain,[53] duration of high-fat feeding, as well as the fat % of the diet (45% of calories from come from fat in our study). Many obesity experiments are performed in male mice that gain more body weight than females in response to HFD.[54] Our experiment is similar to other obesity experiments

with regard to fat mass and fat pad weight (typically a doubling in the obese compared with controls).[51]

Daily running distances were similar in both exercising groups (LFD-E, 10.16±2.98; DIO-E, 9.19±1.94 km/d, $p = 0.5$) (Fig. 1*B*). Other studies[55,56] have shown similar daily running distances with voluntary wheel-based running, but daily distances do vary with regard to mouse strain, sex, and age. At the end of the 6-week experimental period, exercise did not impact weight gain in either LFD or DIO groups (Fig. 1*A*). Perigonadal fat pad weight responded to diet and exercise, higher by 159% in DIO compared with LFD, with an exercise-associated decrement of 22% in LFD and 26% in DIO ($p<0.05$, Fig. 1*E*).

Exercise lowers MAT volume in both lean and obese mice

MAT was quantified via volumetric μCT imaging of the lipid binder, osmium tetroxide.[22,37] Visualization was achieved by superimposing and averaging the μCT images ($n = 10$ per group for pre-exercise images and $n = 6$ per group for post-exercise images) and color labeling of osmium signal according to HU density (Fig. 2*A*). Before initiation of exercise, DIO demonstrated 45% more MAT as measured by MRI compared with LFD ($p<0.05$, Supplemental Fig. S2*B*, $n = 10$ per group). After 6 weeks of exercise, in both sagittal and coronal images, the osmium signal was highest in femurs from DIO groups (Fig. 2*A*), albeit not statistically different (Fig. 2*B*), diverging from our prior finding of higher MAT (normalized to bone volume) in the setting of short-term high-fat feeding.[22]

Both lean and DIO groups responded to exercise with significantly lower MAT: −23% in LFD and −48% in DIO (exercise effect $p<0.05$). In fact, 6 weeks of exercise associated with lower lipid volume in the DIO group to levels equivalent with LFD-E femurs as shown in Fig. 2*B*.

To extend our osmium-μCT analysis using a method that is less toxic to the investigator and one that would allow for *in vivo* imaging assessment, we employed a novel MRI-based approach using a 9.4T scanner to study marrow fat in rodents. Because protons in fat and water have a 3.5 ppm difference in NMR frequency, images of the water content can be separated from images of lipid content. Superimposing these averaged images allows visualization of lipid within bone, similar to the method we have utilized with the bone masking in the osmium-μCT technique. MRI visualization of the marrow lipid shows the same effect of exercise lowering lipid content that was demonstrated with the μCT method (Fig. 2*C, D*) ($p<0.001$). Again, the DIO animal did not have statistically different total MAT, similar to the osmium-μCT method, but the exercise effect to decrease MAT was significant. The Pearson correlation between the osmium-μCT and MRI methods for measuring MAT was statistically significant ($r = 0.645$, $p<0.01$) (Fig. 2*E*). In both the osmium-μCT and MRI methods, we did find that DIO was associated with higher total bone volume. To characterize this alteration in bone size, we measured femoral length, which was not different between LFD and DIO (data not shown). However, we found that DIO mice have slightly larger bones in terms of circumference. With the increase in circumference, there is also an increase in endosteal volume of 35% ($p<0.01$), which was confirmed with μCT.

Exercise shrinks adipocytes in lean and obese mice

Assessment of marrow fat volume cannot determine whether there are more or larger adipocytes in diet and exercise-treated animals. Limitations to defining adipocyte size in any fat depot include the need to accurately contour adipocyte perimeter, which is difficult when cells abut each other and are further subject to fixation artifact (Fig. 3*A*). To overcome this challenge, we determined the average size of clearly demarcated adipocytes within hematoxylin-stained histologic sections using Image J (detailed in Supplemental Fig. S1*B*). To assess variability in cell size, a histogram with Gaussian-fit curves was generated, with each cell fitting in 60-μm^2-wide bins, and, due to the varying number of cells analyzed in each group, the data are represented in percentage of total cells in each bin (LFD, $n = 1101$; LFD-E, $n = 886$; DIO, $n = 563$; DIO-E, $n = 793$). This analysis shows that bone marrow adipocytes in DIO-fed groups were larger than those on the lean diet and that exercise reduced the average size of each adipocyte irrespective, by 19% in LFD and 37% in DIO (Fig. 3*C*). From the area data, the diameter of each cell was calculated, and the same analysis was performed (Supplemental Fig. S1*C, D*), which follows the same trends as found in the area analysis. Exercise did not affect adipocyte number in LFD; however, in DIO exercise associated with a 56% lower adipocyte number (DIO-E versus DIO, $p<0.0001$). Importantly, exercise "normalized" adipocyte size in DIO-E, producing a size similar in dimension to LFD (Fig. 3*C*). Interestingly, there was a significantly lower adipocyte size with exercise in the low-fat-fed animal as well as DIO, suggesting that fat fuel stored in marrow adipocytes is utilized during running exercise. Marrow adipocyte area was 44% higher in the DIO, whereas exercise associated with a reduced marrow adipocyte area: −33% in LFD and −39% in DIO ($p<0.0001$) (Fig. 3*C*).

Exercise was associated with higher trabecular and cortical bone quantity in lean and obese mice

Bone microarchitecture parameters were analyzed by μCT. The pre-exercise 16-week-old baseline controls demonstrated no difference with regard to bone microarchitecture between LFD and DIO groups (Supplemental Table S2, $n = 10$/group). At the end of the 6-week exercise intervention, running exercise, but not diet, affected trabecular bone quantity and quality in the proximal tibial metaphysis. Trabecular bone volume fraction (BV/TV) was higher in exercisers in both LFD and DIO (both by 19%, $p<0.01$, Fig. 4*A*). Although trabecular number (Tb.N) and trabecular separation (Tb.Sp) remained similar between groups, trabecular thickness (Tb.Th) was significantly affected by exercise: 24% higher in LFD-E versus LFD ($p<0.01$) and 48% higher in DIO-E versus DIO ($p<0.0001$) (Fig. 4*A*). DIO associated with lower cortical area fraction (Ct.Ar/Tt.Ar) by 2.4% compared with LFD ($p<0.05$, Fig. 5*B*). Additionally, in DIO versus LFD, the periosteal and endosteal volumes were higher by 15% ($p = 0.01$) and 35% ($p<0.01$), respectively. Thus, obesity resulted in a larger size of bone as well as an additionally higher endosteal cavity volume, resulting in a similar cortical thickness even in a larger animal (schematic overview in Fig. 7). Endosteal volume increases associated with DIO are compensated for by a trend toward increased total cortical area with a small increase in periosteal diameter. This finding suggests the bone marrow cavity in DIO bones expands and that this obesity-driven process is abrogated in the setting of exercise.

Exercise was associated with a cortical thickness 2% higher in LFD and 7% higher in DIO compared with non-exercisers ($p<0.05$ for an exercise effect, Fig. 4*B*). This exercise effect on cortical bone thickness was more significant in obese compared with lean mice. Cortical porosity was not significantly affected, although there was a trend for lower cortical porosity with exercise in LFD (Fig. 4*B*).

Obesity-induced biomechanical changes are reversed with exercise

The rotational moment of inertia (MOI), which is an index of resistance to bending, was +24% higher in DIO ($p<0.05$) in the the YY (Iyy) plane and +37% in the XX (Ixx) plane ($p<0.05$) (Fig. 5*A*). Exercise attenuated pMOI in DIO-E, although the effect was not significant. Stiffness and Young's modulus were quantified through 4-point bending of the tibia: a trend for higher bone stiffness (N/m) was noted in DIO; exercise was additive to this effect (Fig. 5*B*). Thus, DIO was associated with higher stiffness as measured by 4-point bending (resistance to fracture) and polar moment of inertia in the Ixx plane, parameters that point to greater bone quality.[57,58] Exercise generated an even higher 4-point bending stiffness in both LFD and DIO groups.

Marrow fat gene expression supports its function as an energy depot

Total bone mRNA was analyzed to assess for changes in fat and metabolism-associated genes. DIO associated with higher lipid storage marker FSP27 (+80% versus LFD, $p<0.001$), adipose tissue mass regulator LepR (+36% versus LFD, $p<0.01$) (Fig. 6). Perilipin (PLIN) 1 and 5 are involved in lipid droplet growth, and both increase with DIO, PLIN 5 more significantly (PLIN5 +73%, $p<0.05$, versus PLIN 1+54%, $p = 0.08$). That these genes did not return to control levels with exercise might suggest that they represent the number of fat cells in bone. As such, the lower fat mass due to exercise would primarily arise through burning of adipocyte triglyceride. The diet-associated higher PLIN5 suggests that there was increased lipid storage in bone marrow. PLIN 3, which is associated with oxidation of palmitate[33] as well as promoting basal lipolysis,[34] was sensitive to exercise, showing near 100% increases in both exercise groups (LFD-E +92%, DIO-E +109%, $p = 0.01$ for an exercise effect, Fig. 6). MAT was recently found to be a major source of circulating adiponectin;[59] however, bone adiponectin mRNA in our study was not altered by DIO or running (Supplemental Table S1). Other WAT markers, including FASN and aP2, were not significantly affected by diet or exercise (Supplemental Table S1).

Discussion

The physiologic function of marrow fat, in contrast to other fat depots, remains largely unknown. In our previous work, we showed that bone marrow fat rises rapidly after 6 weeks of high-fat feeding, and this rise can be entirely prevented by running exercise.[22] Here we investigated the effects of exercise on long-term obesity-induced marrow fat, utilizing rigorous imaging techniques to quantify adipose tissue volume as well as adipocyte size and number. We found that exercise associated with lower MAT even in the setting of established obesity. Importantly, running exercise caused a significant decrease in the size and number of marrow adipocytes. At the same time, we found that chronic obesity led to larger bone volumes, endosteal volumes (and hence marrow cavity area) and smaller bone area fractions

(Fig. 7). Obese mice responded to running exercise with improved trabecular and cortical bone quantity, thicker cortices, and improved bone quality and stiffness. Overall, obesity and exercise were additive in terms of improving bone quantity (Fig. 4, see Tb.Th, Ct.Th) and quality (Fig. 5*B*, see stiffness). Exercise induction of *PLIN3* in bone indicates an increase in lipolysis and β-oxidation of lipids. These findings indicate that marrow adipocytes shrink during exercise, perhaps even providing fuel for exercise-induced bone formation. This suggests that marrow fat might be tapped as an energy reservoir to promote anabolic adaptations in bone.

Increased fat calories in the diet contribute to expanded MAT volume ahead of increases in visceral white adipose fat depots during short-term high-fat feeding.[22] With established obesity, marrow adipocyte size and number were both significantly larger. Higher lipid as quantified by osmium-μCT and MRI as well as larger fat cell size suggests that marrow adipocytes store lipid similarly to adipocytes located in white adipose depots, by increasing cell size as well as cell number.[60,61] That being said, it is notable that the average adipocyte size in the marrow for LFD, LFD-E, and DIO-E mice was about one-half the size of a peripheral adipocyte on a control or low-fat diet,[62] and for DIO, marrow adipocytes are approximately one-fifth the size of a peripheral adipocyte on a similar high-fat diet.[45] Size differences may be due to local constraints of the skeleton or to phenotypic differences[63] in the progenitor source.[64] The expansion of lipid droplets in the obese bones is further supported by higher *Fsp27*, as mice with adipocyte-specific deletion of *Fsp27* have smaller adipocytes and lower lipid storage capacity.[65] Typically, HFD-fed mice ingest higher total daily calories because of the calorie-dense nature of their diet. Exercising mice have been shown to consume higher daily calories compared with sedentary controls.[22,66,67] Quantification of caloric intake is planned for future studies to further our understanding of energy utilization in the setting of increased (and decreased) MAT.

Exercise leads to lower lipid mass in bone marrow in the setting of control and high-fat diets,[22] PPARγ agonist therapy,[29] and now, as we have shown here, obesity. The reduced size of individual adipocytes within the marrow space suggests that they may provide fuel for exercise and for exercise-induced anabolic adaptations in skeletal tissue. Consistent with this idea is the measured increase in bone mRNA encoding *perilipin 3* (*PLIN3*). Perilipin 3 has been noted to play a role in β-oxidation of lipids in muscle[33] and other tissues,[68,69] as well as in promoting higher rates of basal lipolysis.[34] The exercise induction of *PLIN3* and *Acox1* (which has a role in peroxisomal β-oxidation) supports that MAT contributes to local energy needs during exercise. Of the lipid-droplet-associated perilipin family of proteins, *PLIN3* is recognized as a regulator of lipid oxidation.[33,70] *PLIN3* is positively associated with the 24-hour RQ and palmitate oxidation.[33] *PLIN3* knockdown has been shown to reduce lipid oxidation, and in vitro lipolytic stimulation increases *PLIN3*.[33] In this study, we found that *PLIN3* expression was higher in the tibia of exercising mice, regardless of diet. In addition to increased *PLIN3* indicating an increase in lipid oxidation, the size of marrow adipocytes was significantly smaller in exercising mice, supporting that lipid is utilized during the exercise intervention. *PLIN3* is upregulated in response to exercise in muscle,[69] further supporting its role in β-oxidation in bone. In fact, the obese running mice compared with lean running mice had greater declines in MAT volume, adipocyte size, and adipocyte number, suggesting that they preferentially utilized this energy store. Indeed,

studies indicate that local energy metabolism is critical for osteoblastogenesis/bone formation.[71–73] Conversely, our data suggest that a sedentary and obese state promotes MAT accumulation, a lipid depot that might serve a teleological advantage. Running partially offsets energy costs of thermogenesis, as has been noted in a study of wild weasels,[74] therefore it is possible that the protective effects of running on the mouse skeleton may be due to substitution of exercise for non-shivering thermogenesis to maintain body temperature. We did not find an "exercise dose" effect on marrow fat or bone parameters, which may be because of the fact that the running distance was not significantly different between wheel runners (Supplemental Fig. S4). These data support that increasing exercise duration does not necessarily correlate with additional bone mass, suggesting that exercise bouts could be shortened (or even optimized, inserting rest periods as we have published *in vitro*).[75]

Higher bone quantity, lower MAT, and reduced marrow adipocyte diameter and number along with increased *PLIN3* in the running animals suggest that β-oxidation increases in the skeleton generating fuel for anabolism. Other cells residing in bone (eg, HSC lineage) besides osteoblasts may benefit from this energy source. It should be noted that RBCs rely solely on glucose because they contain no mitochondria, and HSC, with lower mitochondrial mass, also prefer to utilize glucose.[76] Osteoblasts are able to utilize both lipid and glucose as energy sources[77] with fatty acid oxidation accounting for 40% to 80% of total energy requirement.[78]

The study of MAT requires reproducible, quantitative methodologies. Here we validated an image-based method for quantifying lipid in bone in rodents that employs MRI fat map images analyzed via 3D image analysis and normalized to bone volume. The MRI technique was compared with our previously published osmium-μCT method with 3D image analysis[22,29] as well as to quantitative histologic measurements including adipocyte area and diameter. The volumetric MRI method correlates well with our established osmium-μCT method. Because MRI can distinguish between the magnetic resonance signal from lipid in MAT from the usual signal from water, no [toxic] staining is required, and it has the potential to be utilized for longitudinal, in vivo studies of MAT. Additionally, there is no "batch effect," a limitation of osmium staining, thus allowing MAT comparison across different experiments. These imaging methods, however, while both reliable for volumetric quantification of lipid, do not allow assessment of adipocyte number or size. Here we used histological assessment to show that obesity and higher volumetric MAT were associated with an increase in size as well as number of marrow adipocytes. That obesity associated with greater adipocyte size and number[79] and that both measures were lower with exercise as would be expected in other white fat depots[80] is consistent with obesity-induced hypertrophy and hyperplasia of marrow adipocytes.

Importantly, obese mice were quick to participate in voluntary running, running as far and as fast to induce increases in BV/TV that were at least as significant as their lean counterparts. What is particularly notable here is that in the setting of DIO, exercise led to use of fat for fuel, correlating with a reduction in marrow adipocyte size, number, and marrow fat volume to levels not significantly different from lean runners. Extra-marrow fat depot volume—as quantified by total body MRI and by the weight of gonadal fat pads—also responded to DIO

and exercise, similar to the response of marrow fat (increasing in DIO and significantly decreasing in the setting of exercise). Beginning with larger fat stores, this suggests that the marrow fat can be utilized as fuel for the costs of bone formation. This was also the case for the increase in MAT in mice treated with the PPARγ agonist rosiglitazone:[29] PPARγ induced MAT, extending even beyond the diaphysis, but this fat was attenuated by exercise with decreases comparable to control running animals. Interestingly in rosiglitazone-treated mice, intracortical porosity was higher, suggesting a negative effect on bone quality.[29] This may represent a direct effect of the PPARγ agonist on mesenchymal precursors,[81] perhaps to interfere with adaptive remodeling. Interestingly, the increased marrow fat content shown in postmenopausal women was reduced during treatment with teriparatide to induce bone formation.[82]

In addition to emphasizing the physiologic role of MAT in the setting of exercise and obesity, this study also serves to correlate MAT response to that of bone quantity and quality. Several studies show that obesity is associated with higher bone density,[83,84] although data from the Women's Health Initiative suggest that BMD scales with lean mass, rather than total body weight or fat mass.[85] In our mouse study, obese sedentary mice had similar trabecular bone quantity and slightly reduced cortical bone quantity compared with mice fed a control diet (Fig. 4). Biomechanical properties in the Tibial mid-diaphysis were improved in the obese compared with the lean mice. Additionally, although femoral bones were bigger in DIO mice, they had a smaller bone area fraction and circumferentially larger marrow area (Fig. 7), which might suggest that obesity—in the setting of sedentary state—is associated with an increase in endosteal bone resorption. The endosteal volume expansion in DIO mice is compensated by an increase in MOI, resulting in a similar resistance to bending. Interestingly, the same increase in bending resistance is achieved in exercised DIO mice, not by expansion of the polar moments of inertia, but by increasing cortical thickness. Although the periosteal volume remained the same after exercise in the setting of obesity, the endosteal volume was reduced, in what appears an attempt to normalize the shift in bone compromised by obesity. Importantly, the distribution of biomechanical data in the exercise groups have lower standard deviations, perhaps reflecting the ability of exercise or mechanical loading toward regulating bone's mechanical properties or increasing its ability to withstand load across a given surface area. Perhaps exercise and/or mechanical stimuli serve to organize cells and tissues down a predictable pathway of formation (or reduced resorption), whereas negligible mechanical input results in more varied outcomes. The inclusion of mechanical load in the form of exercise reduces the endosteal volume by increasing cortical thickness. B6 mice experience an age-related reduction in trabecular BV/TV as well as an age-related increase in trabecular thickness.[86] Our data demonstrate that both trabecular BV/TV as well as trabecular thickness are significantly higher in exercisers. This could be due to exercise-induced bone formation or to an effect to slow bone loss. Nevertheless, recovering cortical bone area and thickness after exercise highlights its ability to orchestrate more tightly organized bone remodeling processes, independent of bone size.[87]

A limitation of our work includes the use of mice to answer questions about MAT and its relevance to bone health, and yet prior studies in mice confirm that MAT abundance is similar to that of humans in pathologic states including postmenopausal osteoporosis, aging,

and anorexia nervosa.[24] Thus, our data are relevant to the understanding of skeletal health in humans. Additionally, dietary and exercise trials in humans can be fraught with bias, an important factor in pursuing experiments in rodents that illuminate the mechanistic underpinnings of human disease.

In sum, our data beg the question of whether all MAT is equivalent. In comparison to diet-induced increases in MAT, bone fat has historically been associated with decreased bone quantity and strength, as in postmenopausal osteoporosis, anorexia, unloading bone loss, and phosphate restriction,[24,88,89] suggesting an inverse relationship arising out of potential MSC biasing to promote adipocyte rather than osteoblast differentiation. Our data demonstrating loss of lipid in marrow adipocytes in response to running exercise indicate that marrow fat serves as a fuel depot. Further, the presence of marrow fat does not prevent MSC recruitment for adaptive bone formation. It is, however, likely that in pathophysiological conditions such as aging or unloading, where marrow fat is also present, that a loss of an adaptive loop recruiting osteoblasts to remodeling bone surfaces might compromise this energy store. Whether MAT rises because of the inability of osteoblasts to utilize available fuel or because MSC are prevented from entering the osteoblast lineage is an important question for future studies. What is evident here is that DIO results in higher marrow volume, causing the bone to alter its strategy to maintain strength (higher MOI). Exercise reduces MAT, increases local markers of fat utilization, and enables bone quantity/quality to be achieved by a more robust skeleton, rather than a larger one. Exercise appears to drive a more organized form of bone remodeling as a strategic means to accommodate the changes brought on by obesity. Exercise improves bone quantity and quality in LFD and DIO, but the obese exercisers benefited more as they began with an adaptation away from the norm.

Supplementary Material

Refer to Web version on PubMed Central for supplementary material.

Acknowledgments

We recognize and thank Mark Horowitz for osmium staining of mouse femurs.

Grant support: MS: AR062097, P30DK056350; JR: AR066616; JR and CTR: EB014351; GU: P20GM109095.

Biographies

Maya Styner

University of North Carolina at Chapel Hill

Buer Sen

University of North Carolina at Chapel Hill

Zhihui Xie

University of North Carolina at Chapel Hill

Clinton Rubin

Stony Brook University

References

1. Ogden CL, Carroll MD, Kit BK, Flegal KM. Prevalence of childhood and adult obesity in the United States, 2011–2012. JAMA. 2014; 311(8):806–14. [PubMed: 24570244]
2. Clark EM, Ness AR, Tobias JH. Adipose tissue stimulates bone growth in prepubertal children. J Clin Endocrinol Metab. 2006; 91(7):2534–41. [PubMed: 16621904]
3. Sayers A, Tobias JH. Fat mass exerts a greater effect on cortical bone mass in girls than boys. J Clin Endocrinol Metab. 2010; 95(2):699–706. [PubMed: 20008022]
4. Timpson NJ, Sayers A, Davey-Smith G, Tobias JH. How does body fat influence bone mass in childhood? A Mendelian randomization approach. J Bone Miner Res. 2009; 24(3):522–33. [PubMed: 19016587]
5. Reid IR, Ames R, Evans MC, et al. Determinants of total body and regional bone mineral density in normal postmenopausal women—a key role for fat mass. J Clin Endocrinol Metab. 1992; 75(1):45–51. [PubMed: 1619030]
6. Evans AL, Paggiosi MA, Eastell R, Walsh JS. Bone density, microstructure and strength in obese and normal weight men and women in younger and older adulthood. J Bone Miner Res. 2015; 30(5):920–8. [PubMed: 25400253]
7. Finkelstein JS, Lee H, Leder BZ, et al. Gonadal steroid-dependent effects on bone turnover and bone mineral density in men. J Clin Invest. 2016; 126(3):1114–25. [PubMed: 26901812]
8. Gourlay ML, Preisser JS, Hammett-Stabler CA, Renner JB, Rubin J. Follicle-stimulating hormone and bioavailable estradiol are less important than weight and race in determining bone density in younger postmenopausal women. Osteoporos Int. 2011; 22(10):2699–708. [PubMed: 21125395]
9. Case N, Sen B, Thomas JA, et al. Steady and oscillatory fluid flows produce a similar osteogenic phenotype. Calcif Tissue Int. 2011; 88(3):189–97. [PubMed: 21165611]
10. Lecka-Czernik B, Stechschulte LA, Czernik PJ, Dowling AR. High bone mass in adult mice with diet-induced obesity results from a combination of initial increase in bone mass followed by attenuation in bone formation; implications for high bone mass and decreased bone quality in obesity. Mol Cell Endocrinol. 2015; 410:35–41. [PubMed: 25576855]
11. Lavet C, Martin A, Linossier MT, et al. Fat and sucrose intake induces obesity-related bone metabolism disturbances: kinetic and reversibility studies in growing and adult rats. J Bone Miner Res. 2016; 31(1):98–115. [PubMed: 26175082]
12. Cao JJ, Gregoire BR, Gao H. High-fat diet decreases cancellous bone mass but has no effect on cortical bone mass in the tibia in mice. Bone. 2009; 44(6):1097–104. [PubMed: 19264159]

13. Cao JJ, Sun L, Gao H. Diet-induced obesity alters bone remodeling leading to decreased femoral trabecular bone mass in mice. Ann NY Acad Sci. 2010; 1192:292–7. [PubMed: 20392249]
14. Scheller EL, Khoury B, Moller KL, et al. Changes in skeletal integrity and marrow adiposity during high-fat diet and after weight loss. Front Endocrinol (Lausanne). 2016; 7:102. [PubMed: 27512386]
15. Ionova-Martin SS, Do SH, Barth HD, et al. Reduced size-independent mechanical properties of cortical bone in high-fat diet-induced obesity. Bone. 2010; 46(1):217–25. [PubMed: 19853069]
16. Cohen A, Dempster DW, Recker RR, et al. Abdominal fat is associated with lower bone formation and inferior bone quality in healthy premenopausal women: a transiliac bone biopsy study. J Clin Endocrinol Metab. 2013; 98(6):2562–72. [PubMed: 23515452]
17. Sornay-Rendu E, Boutroy S, Vilayphiou N, Claustrat B, Chapurlat R. In obese postmenopausal women, bone microarchitecture and strength are not commensurate to greater body weight. The OFELY study. J Bone Miner Res. 2013; 28(7):1679–87. [PubMed: 23371055]
18. Meyer HE, Willett WC, Flint AJ, Feskanich D. Abdominal obesity and hip fracture: results from the Nurses' Health Study and the Health Professionals Follow-up Study. Osteoporos Int. 2016; 27(6):2127–36. [PubMed: 26849456]
19. Compston JE, Flahive J, Hosmer DW, et al. Relationship of weight, height, and body mass index with fracture risk at different sites in postmenopausal women: the Global Longitudinal Study of Osteoporosis in Women (GLOW). J Bone Miner Res. 2014; 29(2):487–93. [PubMed: 23873741]
20. Compston J. Obesity and bone. Current Osteoporos Rep. 2013; 11(1):30–5.
21. Compston JE, Watts NB, Chapurlat R, et al. Obesity is not protective against fracture in postmenopausal women: GLOW. Am J Med. 2011; 124(11):1043–50. [PubMed: 22017783]
22. Styner M, Thompson WR, Galior K, et al. Bone marrow fat accumulation accelerated by high fat diet is suppressed by exercise. Bone. 2014; 64C:39–46.
23. Lecka-Czernik B, Stechschulte LA. Bone and fat: a relationship of different shades. Arch Biochem Biophys. 2014; 561:124–9. [PubMed: 24956594]
24. Paccou J, Hardouin P, Cotten A, Penel G, Cortet B. The role of bone marrow fat in skeletal health: usefulness and perspectives for clinicians. J Clin Endocrinol Metab. 2015; 100(10):3613–21. [PubMed: 26244490]
25. Schafer AL, Li X, Schwartz AV, et al. Changes in vertebral bone marrow fat and bone mass after gastric bypass surgery: a pilot study. Bone. 2015; 74:140–5. [PubMed: 25603463]
26. Pagnotti GM, Styner M. Exercise regulation of marrow adipose tissue. Front Endocrinol (Lausanne). 2016; 7:94. [PubMed: 27471493]
27. Garaulet M, Hernandez-Morante JJ, Lujan J, Tebar FJ, Zamora S. Relationship between fat cell size and number and fatty acid composition in adipose tissue from different fat depots in overweight/obese humans. Int J Obes (Lond). 2006; 30(6):899–905. [PubMed: 16446749]
28. Bredella MA, Torriani M, Ghomi RH, et al. Vertebral bone marrow fat is positively associated with visceral fat and inversely associated with IGF-1 in obese women. Obesity (Silver Spring). 2011; 19(1):49–53. [PubMed: 20467419]
29. Styner M, Pagnotti GM, Galior K, et al. Exercise regulation of marrow fat in the setting of PPARgamma agonist treatment in female C57BL/6 mice. Endocrinology. 2015; 156(8):2753–61. [PubMed: 26052898]
30. Srinivasan S, Agans SC, King KA, Moy NY, Poliachik SL, Gross TS. Enabling bone formation in the aged skeleton via rest-inserted mechanical loading. Bone. 2003; 33(6):946–55. [PubMed: 14678854]
31. Srinivasan S. Enabling bone formation in the aged skeleton via restinserted mechanical loading. Bone. 2003; 33(6):946–55. [PubMed: 14678854]
32. Yeh JK, Liu CC, Aloia JF. Effects of exercise and immobilization on bone formation and resorption in young rats. Am J Physiol. 1993; 264(2 Pt 1):E182–9. [PubMed: 8447384]
33. Covington JD, Noland RC, Hebert RC, et al. Perilipin 3 differentially regulates skeletal muscle lipid oxidation in active, sedentary, and type 2 diabetic males. J Clin Endocrinol Metab. 2015; 100(10):3683–92. [PubMed: 26171795]

34. Patel S, Yang W, Kozusko K, Saudek V, Savage DB. Perilipins 2 and 3 lack a carboxy-terminal domain present in perilipin 1 involved in sequestering ABHD5 and suppressing basal lipolysis. Proc Natl Acad Sci U S A. 2014; 111(25):9163–8. [PubMed: 24927580]
35. Willis MS, Min J-N, Wang S, et al. Carboxyl terminus of Hsp70-interacting protein (CHIP) is required to modulate cardiac hypertrophy and attenuate autophagy during exercise. Cell Biochem Funct. 2013; 31(8):724–35. [PubMed: 23553918]
36. Ellis JM, Li LO, Wu PC, et al. Adipose acyl-CoA synthetase-1 directs fatty acids toward beta-oxidation and is required for cold thermogenesis. Cell Metab. 2010; 12(1):53–64. [PubMed: 20620995]
37. Scheller EL, Troiano N, Vanhoutan JN, et al. Use of osmium tetroxide staining with microcomputerized tomography to visualize and quantify bone marrow adipose tissue in vivo. Methods Enzymol. 2014; 537:123–39. [PubMed: 24480344]
38. Fedorov A, Beichel R, Kalpathy-Cramer J, et al. 3D Slicer as an image computing platform for the Quantitative Imaging Network. Magn Reson Imaging. 2012; 30(9):1323–41. [PubMed: 22770690]
39. Yushkevich PA, Piven J, Hazlett HC, et al. User-guided 3D active contour segmentation of anatomical structures: significantly improved efficiency and reliability. Neuroimage. 2006; 31(3): 1116–28. [PubMed: 16545965]
40. Schreiber JJ, Anderson PA, Rosas HG, Buchholz AL, Au AG. Hounsfield units for assessing bone mineral density and strength: a tool for osteoporosis management. J Bone Joint Surg Am. 2011; 93(11):1057–63. [PubMed: 21655899]
41. Fretz JA, Nelson T, Xi Y, Adams DJ, Rosen CJ, Horowitz MC. Altered metabolism and lipodystrophy in the early B-cell factor 1-deficient mouse. Endocrinology. 2010; 151(4):1611–21. [PubMed: 20172967]
42. Joshi S, Davis B, Jomier M, Gerig G. Unbiased diffeomorphic atlas construction for computational anatomy. Neuroimage. 2004; 23(Suppl 1):S151–60. [PubMed: 15501084]
43. Avants BB, Tustison NJ, Song G, Cook PA, Klein A, Gee JC. A reproducible evaluation of ANTs similarity metric performance in brain image registration. Neuroimage. 2011; 54(3):2033–44. [PubMed: 20851191]
44. Longobardi L, Li T, Myers TJ, et al. TGF-beta type II receptor/MCP-5 axis: at the crossroad between joint and growth plate development. Dev Cell. 2012; 23(1):71–81. [PubMed: 22814601]
45. Parlee SD, Lentz SI, Mori H, MacDougald OA. Quantifying size and number of adipocytes in adipose tissue. Methods Enzymol. 2014; 537:93–122. [PubMed: 24480343]
46. Schneider CA, Rasband WS, Eliceiri KW. NIH Image to ImageJ: 25 years of image analysis. Nat Methods. 2012; 9:671–675. [PubMed: 22930834]
47. Pagnotti GM, Adler BJ, Green DE, et al. Low magnitude mechanical signals mitigate osteopenia without compromising longevity in an aged murine model of spontaneous granulosa cell ovarian cancer. Bone. 2012; 51(3):570–7. [PubMed: 22584009]
48. Gross TS, Rubin CT. Uniformity of resorptive bone loss induced by disuse. J Orthop Res. 1995; 13(5):708–14. [PubMed: 7472749]
49. Qin Y-X, Lin W, Rubin C. The pathway of bone fluid flow as defined by in vivo intramedullary pressure and streaming potential measurements. Ann Biomed Eng. 2002; 30(5):693–702. [PubMed: 12108843]
50. Vashishth D. Small animal bone biomechanics. Bone. 2008; 43(5):794–7. [PubMed: 18672104]
51. Brodt MD, Ellis CB, Silva MJ. Growing C57Bl/6 mice increase whole bone mechanical properties by increasing geometric and material properties. J Bone Miner Res. 1999; 14(12):2159–66. [PubMed: 10620076]
52. Montgomery MK, Hallahan NL, Brown SH, et al. Mouse strain-dependent variation in obesity and glucose homeostasis in response to high-fat feeding. Diabetologia. 2013; 56(5):1129–39. [PubMed: 23423668]
53. Heiker JT, Kunath A, Kosacka J, et al. Identification of genetic loci associated with different responses to high-fat diet-induced obesity in C57BL/6N and C57BL/6J substrains. Physiol Genomics. 2014; 46(11):377–84. [PubMed: 24692188]

54. Villena JA, Choi CS, Wang Y, et al. Resistance to high-fat diet-induced obesity but exacerbated insulin resistance in mice overexpressing preadipocyte factor-1 (Pref-1): a new model of partial lipodystrophy. Diabetes. 2008; 57(12):3258–66. [PubMed: 18835937]
55. Hayes A, Williams DA. Beneficial effects of voluntary wheel running on the properties of dystrophic mouse muscle. J Appl Physiol. 1996; 80(2):670–9. [PubMed: 8929614]
56. Waters RE, Rotevatn S, Li P, Annex BH, Yan Z. Voluntary running induces fiber type-specific angiogenesis in mouse skeletal muscle. Am J Physiol Cell Physiol. 2004; 287(5):C1342–8. [PubMed: 15253894]
57. Seeman E, Delmas PD. Bone quality—the material and structural basis of bone strength and fragility. N Engl J Med. 2006; 354(21):2250–61. [PubMed: 16723616]
58. Donnelly E. Methods for assessing bone quality: a review. Clin Orthop Relat Res. 2011; 469(8): 2128–38. [PubMed: 21116752]
59. Cawthorn WP, Scheller EL, Learman BS, et al. Bone marrow adipose tissue is an endocrine organ that contributes to increased circulating adiponectin during caloric restriction. Cell Metab. 2014; 20(2):368–75. [PubMed: 24998914]
60. Heinonen S, Saarinen L, Naukkarinen J, et al. Adipocyte morphology and implications for metabolic derangements in acquired obesity. Int J Obes (Lond). 2014; 38(11):1423–31. [PubMed: 24549139]
61. Spalding KL, Arner E, Westermark PO, et al. Dynamics of fat cell turnover in humans. Nature. 2008; 453(7196):783–7. [PubMed: 18454136]
62. Fabbiano S, Suarez-Zamorano N, Rigo D, et al. Caloric restriction leads to browning of white adipose tissue through type 2 immune signaling. Cell Metab. 2016; 24(3):434–46. [PubMed: 27568549]
63. Krings A, Rahman S, Huang S, Lu Y, Czernik PJ, Lecka-Czernik B. Bone marrow fat has brown adipose tissue characteristics, which are attenuated with aging and diabetes. Bone. 2012; 50(2): 546–52. [PubMed: 21723971]
64. Gavin KM, Gutman JA, Kohrt WM, et al. De novo generation of adipocytes from circulating progenitor cells in mouse and human adipose tissue. FASEB J. 2016; 30(3):1096–108. [PubMed: 26581599]
65. Tanaka N, Takahashi S, Matsubara T, et al. Adipocyte-specific disruption of fat-specific protein 27 causes hepatosteatosis and insulin resistance in high-fat diet-fed mice. J Biol Chem. 2015; 290(5): 3092–105. [PubMed: 25477509]
66. Jung DY, Ko HJ, Lichtman EI, et al. Short-term weight loss attenuates local tissue inflammation and improves insulin sensitivity without affecting adipose inflammation in obese mice. Am J Physiol Endocrinol Metab. 2013; 304(9):E964–76. [PubMed: 23482446]
67. Evans CC, LePard KJ, Kwak JW, et al. Exercise prevents weight gain and alters the gut microbiota in a mouse model of high fat diet-induced obesity. PloS One. 2014; 9(3):e92193. [PubMed: 24670791]
68. Soni KG, Mardones GA, Sougrat R, Smirnova E, Jackson CL, Bonifacino JS. Coatomer-dependent protein delivery to lipid droplets. J Cell Sci. 2009; 122(Pt 11):1834–41. [PubMed: 19461073]
69. Ellong EN, Soni KG, Bui QT, Sougrat R, Golinelli-Cohen MP, Jackson CL. Interaction between the triglyceride lipase ATGL and the Arf1 activator GBF1. PloS One. 2011; 6(7):e21889. [PubMed: 21789191]
70. Louche K, Badin PM, Montastier E, et al. Endurance exercise training up-regulates lipolytic proteins and reduces triglyceride content in skeletal muscle of obese subjects. J Clin Endocrinol Metab. 2013; 98(12):4863–71. [PubMed: 24178794]
71. Esen E, Chen J, Karner CM, Okunade AL, Patterson BW, Long F. WNT-LRP5 signaling induces Warburg effect through mTORC2 activation during osteoblast differentiation. Cell Metab. 2013; 17(5):745–55. [PubMed: 23623748]
72. Karner CM, Esen E, Okunade AL, Patterson BW, Long F. Increased glutamine catabolism mediates bone anabolism in response to WNT signaling. J Clin Endocrinol Metab. 2015; 125(2): 551–62.

73. Bollag RJ, Zhong Q, Phillips P, et al. Osteoblast-derived cells express functional glucose-dependent insulinotropic peptide receptors. Endocrinology. 2000; 141(3):1228–35. [PubMed: 10698200]
74. Chappell MA, Szafranska PA, Zub K, Konarzewski M. The energy cost of voluntary running in the weasel Mustela nivalis. J Exp Biol. 2013; 216(Pt 4):578–86. [PubMed: 23125341]
75. Sen B, Xie Z, Case N, Styner M, Rubin CT, Rubin J. Mechanical signal influence on mesenchymal stem cell fate is enhanced by incorporation of refractory periods into the loading regimen. J Biomech. 2011; 44(4):593–9. [PubMed: 21130997]
76. Shyh-Chang N, Daley GQ, Cantley LC. Stem cell metabolism in tissue development and aging. Development. 2013; 140(12):2535–47. [PubMed: 23715547]
77. Frey JL, Li Z, Ellis JM, et al. Wnt-Lrp5 signaling regulates fatty acid metabolism in the osteoblast. Mol Cell Biol. 2015; 35(11):1979–91. [PubMed: 25802278]
78. Adamek G, Felix R, Guenther HL, Fleisch H. Fatty acid oxidation in bone tissue and bone cells in culture. Characterization and hormonal influences. Biochem J. 1987; 248(1):129–37. [PubMed: 3325035]
79. Hirsch J, Batchelor B. Adipose tissue cellularity in human obesity. J Clin Endocrinol Metab. 1976; 5(2):299–311.
80. Gollisch KS, Brandauer J, Jessen N, et al. Effects of exercise training on subcutaneous and visceral adipose tissue in normal- and high-fat diet-fed rats. Am J Physiol Endocrinol Metab. 2009; 297(2):E495–504. [PubMed: 19491293]
81. Sulston RJ, Learman BS, Zhang B, et al. Increased circulating adiponectin in response to thiazolidinediones: investigating the role of bone marrow adipose tissue. Front Endocrinol (Lausanne). 2016; 7:128. [PubMed: 27708617]
82. Yang Y, Luo X, Xie X, et al. Influences of teriparatide administration on marrow fat content in postmenopausal osteopenic women using MR spectroscopy. Climacteric. 2016; 19(3):285–91. [PubMed: 26744910]
83. Shen J, Leslie WD, Nielson CM, Majumdar SR, Morin SN, Orwoll ES. Associations of body mass index with incident fractures and hip structural parameters in a large Canadian cohort. J Clin Endocrinol Metab. 2016; 101(2):476–84. [PubMed: 26670128]
84. Turner RT, Kalra SP, Wong CP, et al. Peripheral leptin regulates bone formation. J Bone Miner Res. 2013; 28(1):22–34. [PubMed: 22887758]
85. Beck TJ, Petit MA, Wu G, LeBoff MS, Cauley JA, Chen Z. Does obesity really make the femur stronger? BMD, geometry, and fracture incidence in the women's health initiative-observational study. J Bone Miner Res. 2009; 24(8):1369–79. [PubMed: 19292617]
86. Glatt V, Canalis E, Stadmeyer L, Bouxsein ML. Age-related changes in trabecular architecture differ in female and male C57BL/6J mice. J Bone Miner Res. 2007; 22(8):1197–207. [PubMed: 17488199]
87. van der Meulen MC, Jepsen KJ, Mikic B. Understanding bone strength: size isn't everything. Bone. 2001; 29(2):101–4. [PubMed: 11502469]
88. Gupta S, Vijayaraghavan S, Uzer G, Judex S. Multiple exposures to unloading decrease bone's responsivity but compound skeletal losses in C57BL/6 mice. Am J Physiol Regul Integr Comp Physiol. 2012; 303(2):R159–67. [PubMed: 22592559]
89. Ko FC, Martins JS, Reddy P, et al. Acute phosphate restriction impairs bone formation and increases marrow adipose tissue in growing mice. J Bone Miner Res. 2016; 31(12):2204–14. [PubMed: 27324177]

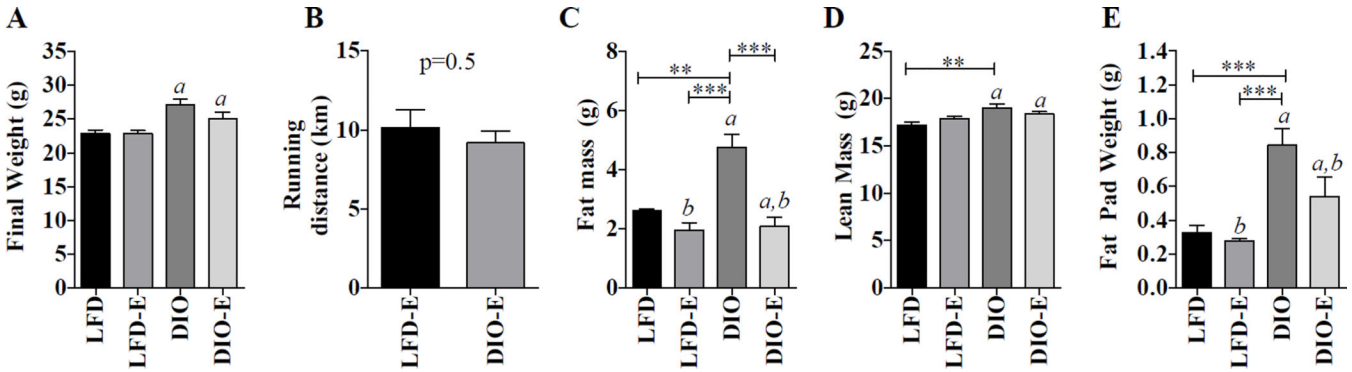

Fig. 1.

Exercise reduces fat mass. C57BL/6 mice were fed either a control (LFD) or high-fat diet (DIO). After 3 months on each diet, 16-week-old mice were divided into runners (LFD-E, DIO-E) versus non-runners (LFD, DIO). (*A*) Final weights of each group. (*B*) Average running distance. (*C*) Total body fat mass and (*D*) lean mass as measured by MRI. (*E*) Weight of perigonadal fat pad. Results are expressed as mean±SEM. a, Significant main effect due to diet by 2- way ANOVA; b, significant main effect due to exercise by 2-way ANOVA. Interaction value was significant ($p<0.01$) for fat mass by 2-way ANOVA. Significance for between-group comparisons: *$p<0.05$; **$p<0.01$; ***$p<0.001$; ****$p<0.0001$.

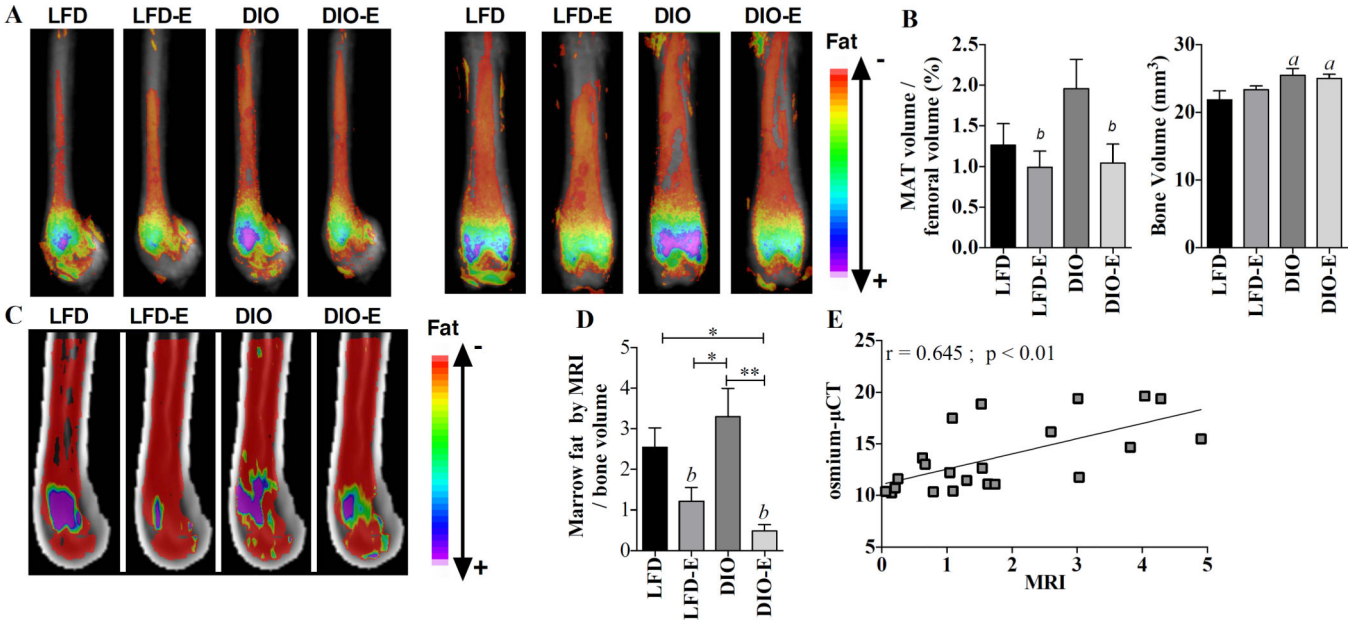

Fig. 2.

Exercise lowers MAT volume in both lean and obese mice. (*A*) Visualization of osmium stain by µCT in sagittal (left) and coronal (right) planes of the femur; $n = 7$/group, each image represents 7 images superimposed on each other. (*B*) Quantification of the bone volume and fat volume normalized to bone as measured by µCT. (*C*) Visualization of MAT measured by MRI; $n = 6$ per group, each image represents 6 images superimposed on each other. (*D*) Quantification of marrow fat volume by MRI normalized to bone volume. (*E*) Correlation of osmium-µCT quantification method of quantification to MRI method. Interaction values by 2-way ANOVA were non-significant. Between-group significance expressed per Fig. 1 legend.

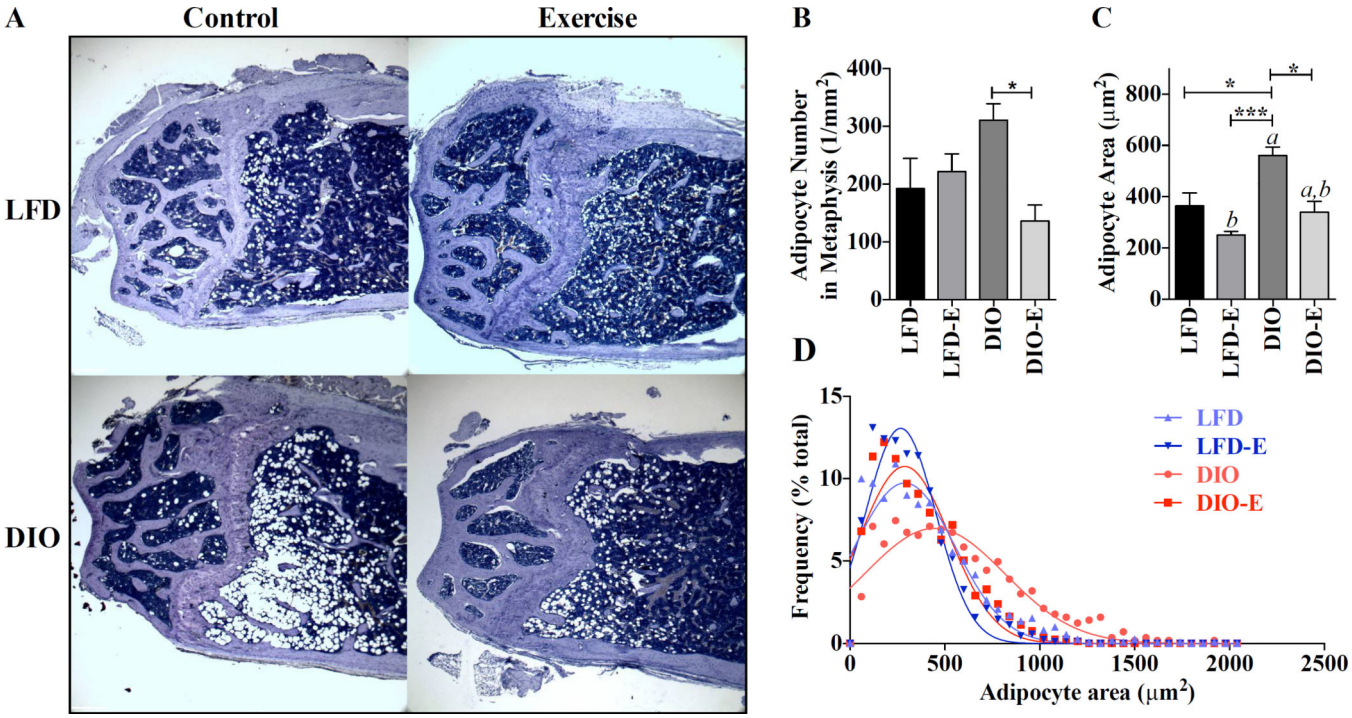

Fig. 3.

DIO increase in marrow adipocyte size is reversed by exercise. Adipocyte size was assessed in high-power field images of the femoral metaphysis. (*A*) Representative images for each group. (*B*) Number of adipocytes per square millimeter. (*C, D*) Area of adipocytes represented as both mean±SEM and as Gaussian fit histogram (LFD, $n = 1101$; LFD-E, $n = 886$; DIO, $n = 563$; DIO-E, $n = 793$ adipocytes); interaction value was solely significant ($p<0.05$) for adipocyte number by 2-way ANOVA. Between-group significance expressed per Fig. 1 legend.

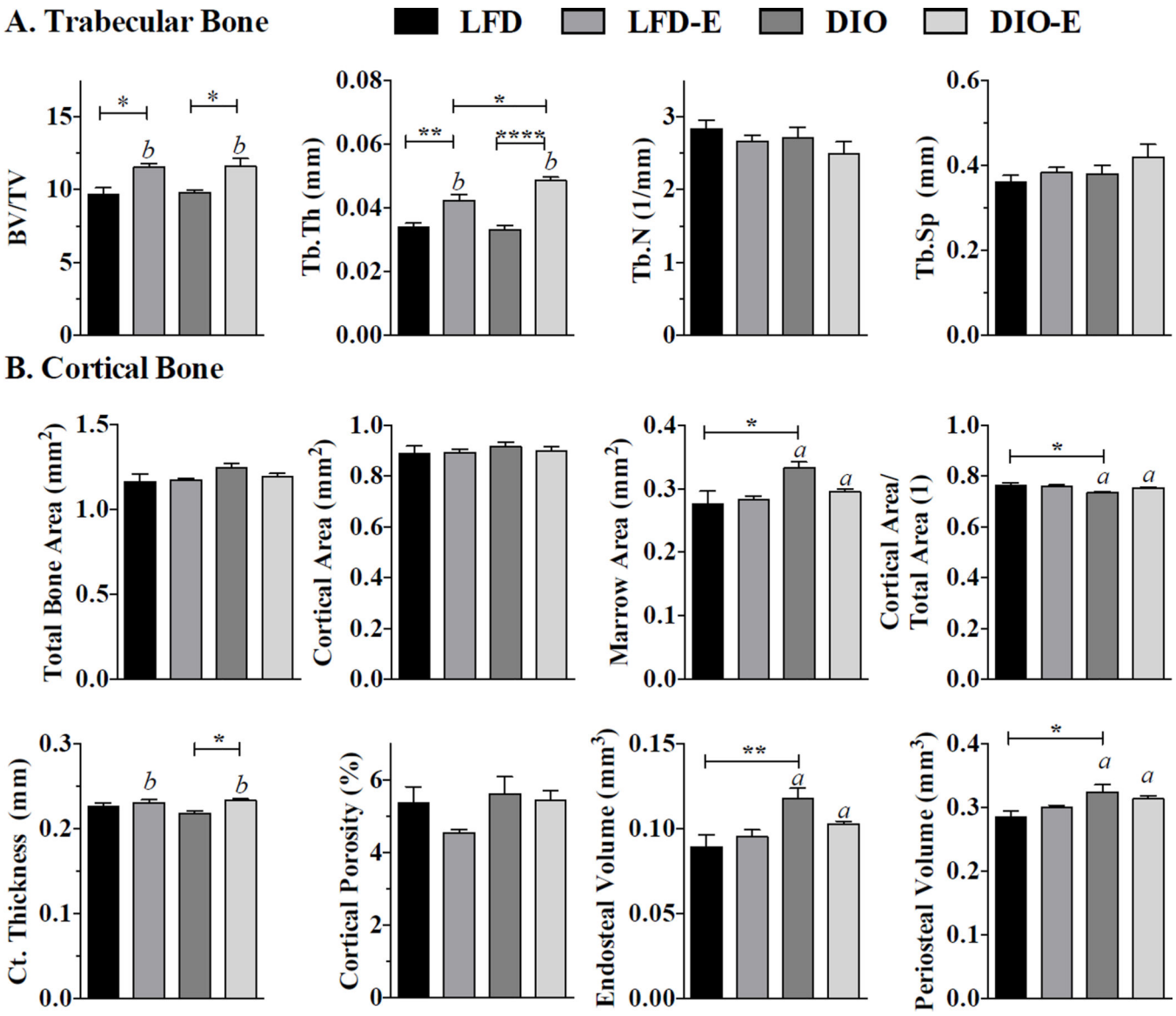

Fig. 4.

Exercise increases trabecular bone thickness more significantly in obese than lean mice. Bone microarchitecture parameters analyzed by μCT. (*A*) Trabecular bone parameters, including bone volume fraction (BV/TV), trabecular thickness (Tb.Th), trabecular number (Tb.N), and trabecular spacing (Tb. Sp), were measured in the tibial proximal metaphysis via μCT. (*B*) Cortical bone parameters, including marrow cavity area, cortical bone area fraction, cortical thickness, cortical porosity, endosteal volume, and periosteal volume, were measured in the tibial mid-diaphysis; interaction values by 2-way ANOVA were non-significant. Between-group significance expressed per Fig. 1 legend.

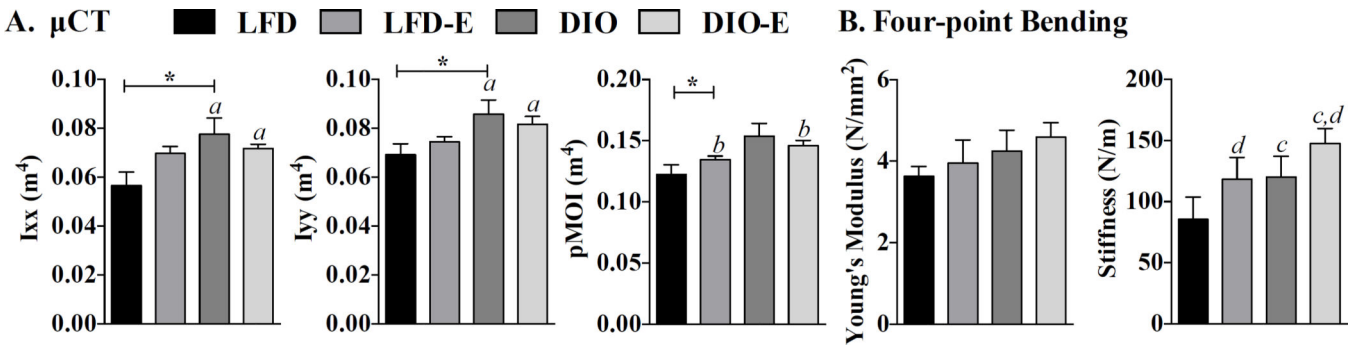

Fig. 5.

Obesity-induced biomechanical changes are reversed with exercise. Biomechanical testing performed by µCT and 4-point bending. (*A*) Moment of inertia values (Ixx, Iyy, and polar moment of inertia) measured by µCT. (*B*) Bone elasticity (Young's modulus) and stiffness as measured by 4-point bending; interaction values by 2-way ANOVA were non-significant. a, Significant main effect due to diet by 2-way ANOVA; b, significant main effect due to exercise by 2-way ANOVA; c, d trend due to diet and exercise, respectively. Between-group significance expressed per Fig. 1 legend.

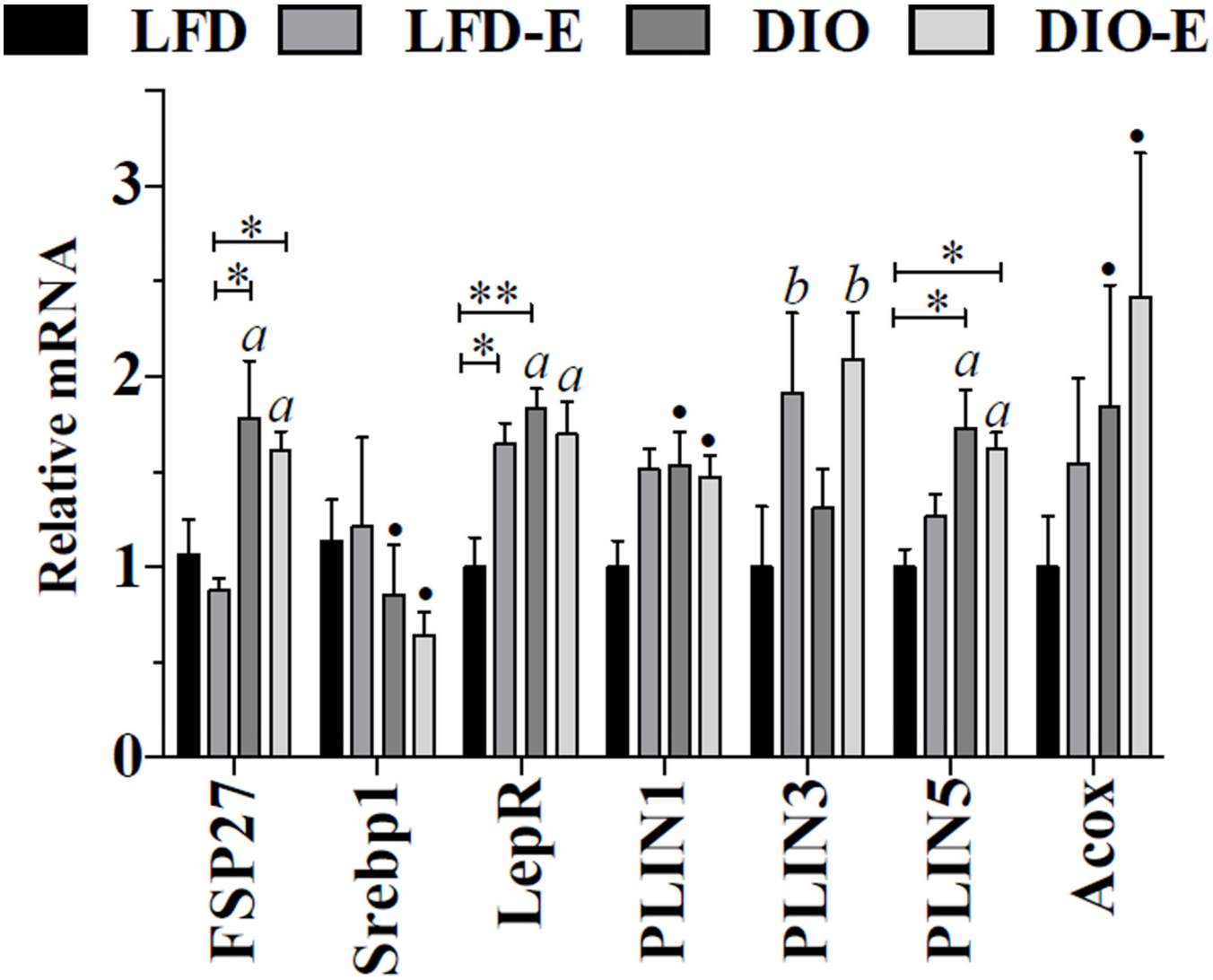

Fig. 6.

Marrow fat gene expression supports its use as a local energy depot. Whole tibia mRNA expression analysis was performed for white fat markers and the lipid droplet associated perilipin family (n = 6/ group). Interaction value was solely significant (p<0.05) for *PLIN1* by 2- way ANOVA. a, Significant main effect due to diet by 2-way ANOVA; b, significant main effect due to exercise by 2-way ANOVA; ● trend; between-group significance expressed per Fig. 1 legend.

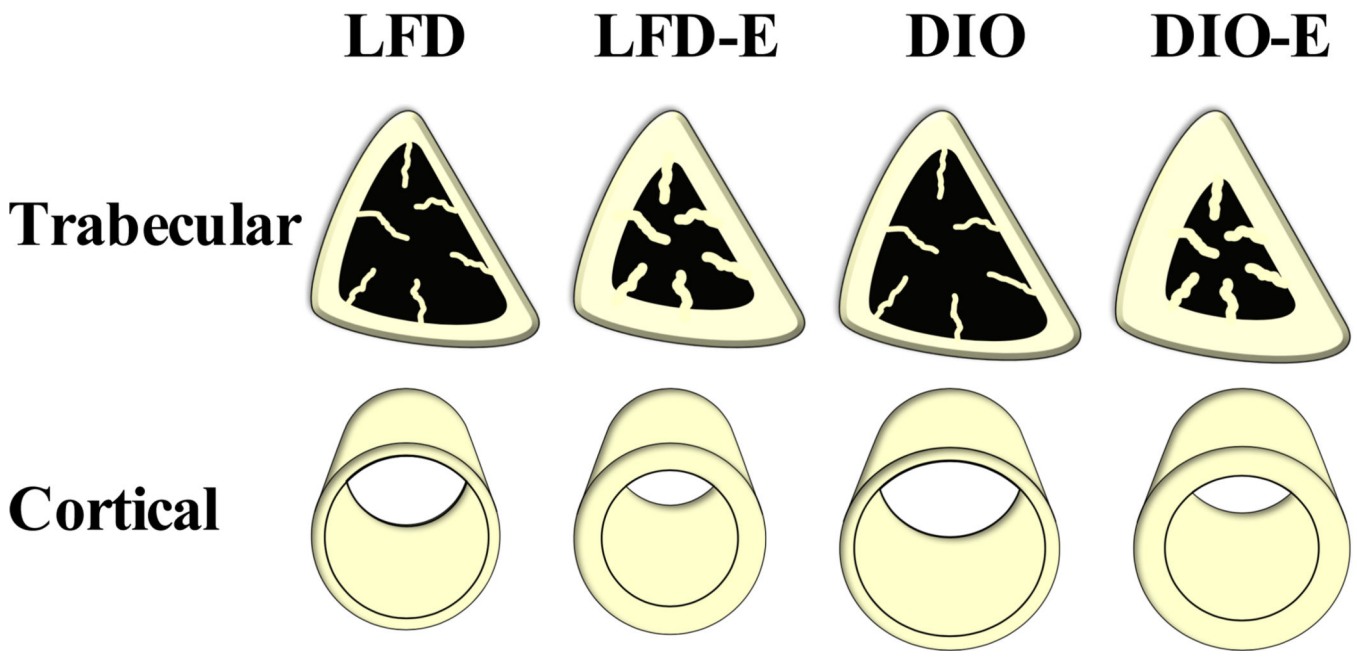

Fig. 7.

Both obesity and exercise impact biomechanical properties of bone. Schematic of biomechanical and microarchitectural effects of diet and exercise on bone.